Journal of the Korean Ceramic Society
Vol. 39, No. 11, pp. 1017~1022, 2002.

$(Ba_{1-x}Ca_x)(Ti_{1-y}Zr_y)O_3$ Powder Synthesis Via Hydrothermal Treatment

Byung-Hyun Park, Kyoon Choi†, Eui-Seok Choi and Jong-Hee Kim*

Korea Institute of Ceramic Engineering and Technology, Seoul 153-023, Korea
**Samsung Electro-Mechanics, Suwon 442-743, Korea*
(Received September 16, 2002; Accepted October 2, 2002)

ABSTRACT

$(Ba_{1-x}Ca_x)(Ti_{1-y}Zr_y)O_3$(BCTZ) powders for the Ni-electrode Multilayer Ceramic Capacitor(MLCC) were synthesized via hydrothermal treatment using mixed aqueous solutions of $BaCl_2 \cdot 2H_2O$, $Ca(NO_3)_2 \cdot 4H_2O$, $ZrOCl_2 \cdot 8H_2O$ and $TiCl_4$. Two component and three component systems were also extensively studied for basic data. BT, CT and BZ powders were crystalline but CZ was determined to be amorphous under the same synthetic condition. In BTZ system, Zr and Ti were completely soluble and Ca would be substituted for Ba up to ~6 mol% in BCT. The submicron-sized $(Ba_{0.95}Ca_{0.05})(Ti_{0.80}Zr_{0.20})O_3$ powder of the target composition was successfully synthesized at 150°C for 12 h.

Key words : $BaTiO_3$, Powder synthesis, Hydrothermal treatment, MLCC

1. Introduction

The dielectric ceramics in Multilayer Ceramic Capacitor(MLCC) have been cofired with internal electrodes of expensive palladium or palladium silver alloys.[1] After decades of research and development,[2] the manufacturers of MLCC are now capable of replacing the expensive noble metals with cheaper base metals such as nickel.[3-6] However, in this case, the dielectrics should be cofired with Base Metal Electrode(BME)[4] in a reducing atmosphere to prevent the oxidation of the internal electrodes. During the firing in a reducing atmosphere, large amount of ionized oxygen vacancies and electrons are formed, which, in turn, give rise to high electric conductivity of the dielectric ceramics. These free electrons are harmful to the performance of MLCC; therefore, they should be trapped by doping of an adequate dopant.[7,8]

As long as the number of oxygen vacancies is smaller than that of acceptors, the dielectrics remain in an insulating state. For this reason, manufacturers of BME-MLCC make use of calcium ions on Ti-sites which have been reported as being very strong acceptors.[9] Han *et al.*[4] found that Ca^{2+} ions that are well known as the A-site substituent may also enter the B-site of BCTZ when the number of Ba and Ca ions exceed those of Ti and Zr. Zhuang *et al.*[10] studied the effect of Ca-acceptors on the conductivity and dielectric properties of $BaTiO_3$. They observed the decrease of the tetragonal distortion of the perovskite unit cell and the subsequent lowering of the Curie point, Tc, with incorporation of Ca ions on B-sites in $BaTiO_3$. Henning *et al.*[11] reported the maximum solubility of ~2% Ca ions on B-sites in $BaTiO_3$.

$(Ba_{0.95}Ca_{0.05})(Ti_{0.80}Zr_{0.20})O_3$ is our target composition of high permittivity that is often expressed as Y5V. Hydrothermal processing is superior to the solid-state synthesis in the standpoint of sinterability and purity because the crystalline powders are directly synthesized in aqueous solutions. Therefore, the high temperature calcination is not necessary and the subsequent milling process can be omitted.[12-14] The hydrothermally synthesized powders have a regular shape[15-17] with a narrow particle size distribution which are very desirable for sinterability. Hydrothermal synthesis has been widely investigated but, to our knowledge, no study on the hydrothermal synthesis of crystalline BCTZ powders has been reported. The main objective of this research is to confirm the possibility of BCTZ powder synthesis via hydrothermal treatment.

2. Experimental Procedures

2.1. Starting Materials

$BaCl_2 \cdot 2H_2O$ (Junsei Chemical Co., Ltd.), $Ca(NO_3)_2 \cdot 4H_2O$ (Hayashi Pure Chemical Industries, Ltd.), $ZrOCl_2 \cdot 8H_2O$ (Junsei Chemical Co., Ltd.) and $TiCl_4$ (Junsei Chemical Co., Ltd.) were used as source materials. NH_4OH (Wako pure chemical industries, Ltd.) and KOH (Shinyo pure chemicals Co., Ltd.) were used as precipitation agent and pH control agent, respectively.

2.2. Preparation of Starting Solutions

Titanium tetrachloride was slowly added to ice-cold distilled water, which was constantly stirred in a 300 ml volumetric flask. The solution became somewhat turbid during the dissolution step but gradually clean up within approximately 30 min, while the temperature of the solution rose to room temperature (~20°C). The final concentration of the

†Corresponding author : Kyoon Choi
E-mail : knchoi@kicet.re.kr
Tel : +82-2-3282-2454 Fax : +82-2-3282-2418

$TiCl_4$ stock solution was adjusted to 1.0 M. This stock solution was held for 24 h before use.

2.3. Preparation of Precursor Suspensions and Hydrothermal Treatment

For the preparation of barium and titanium mixed solution, 30 ml of 1.0 M $TiCl_4$ solution equivalent to 0.03 mol Ti were added to a teflon container of 75 ml. Then 0.03 mole of Ba in the form of $BaCl_2 \cdot 2H_2O$ was dissolved in the $TiCl_4$ solution. To prepare the mixed suspension, NH_4OH was added to the mixed solution until pH value was reached to 9. pH value was adjusted to 13 by addition of KOH. The total volume of the suspensions became 65 ml before hydrothermal treatment. Other suspensions were also made under the same condition. Each suspension was sealed in the teflon container and then placed in a stainless steel jar. The hydrothermal treatment was performed in an oven at the temperature range of 130–210°C for 12 h. The synthesized powders were repeatedly washed with distilled water and dried in an oven at 120°C for 12 h.

The phase identification of synthesized powders was determined by X-Ray Diffractometer(XRD, MAC Science Co. Ltd., Japan) over 2θ range of 10~70° at a scan rate of 4°/min. Morphology and size of the particles were determined using a Scanning Electron Microscope(SEM, JEOL, JSM-6700F).

3. Results and Discussion

3.1. Hydrothermal Synthesis of 2-component Systems

Fig. 1 is the XRD patterns of the powders synthesized hydrothermally from various suspensions at 210°C for 12 h. Crystalline phases of $BaTiO_3$, $BaZrO_3$ and $CaTiO_3$ were obtained while $CaZrO_3$ remained amorphous. The micro-

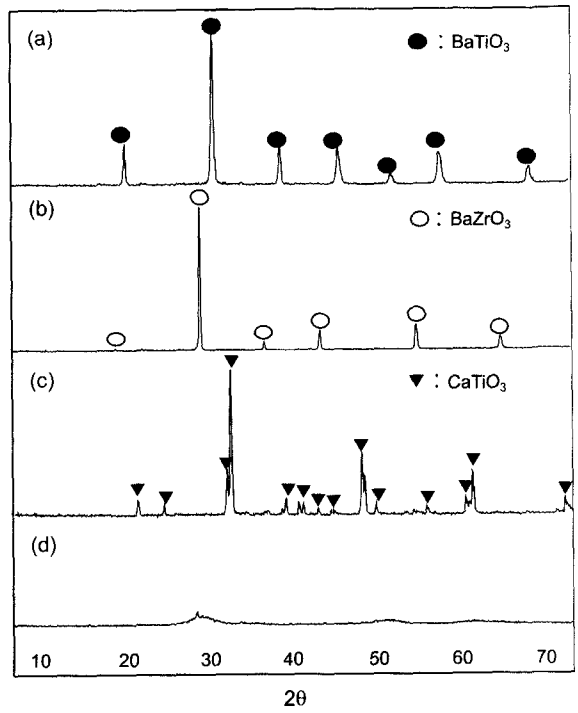

Fig. 1. XRD patterns of (a) $BaTiO_3$, (b) $BaZrO_3$, (c) $CaTiO_3$ and (d) $CaZrO_3$ powders hydrothermally synthesized at 210°C for 12 h.

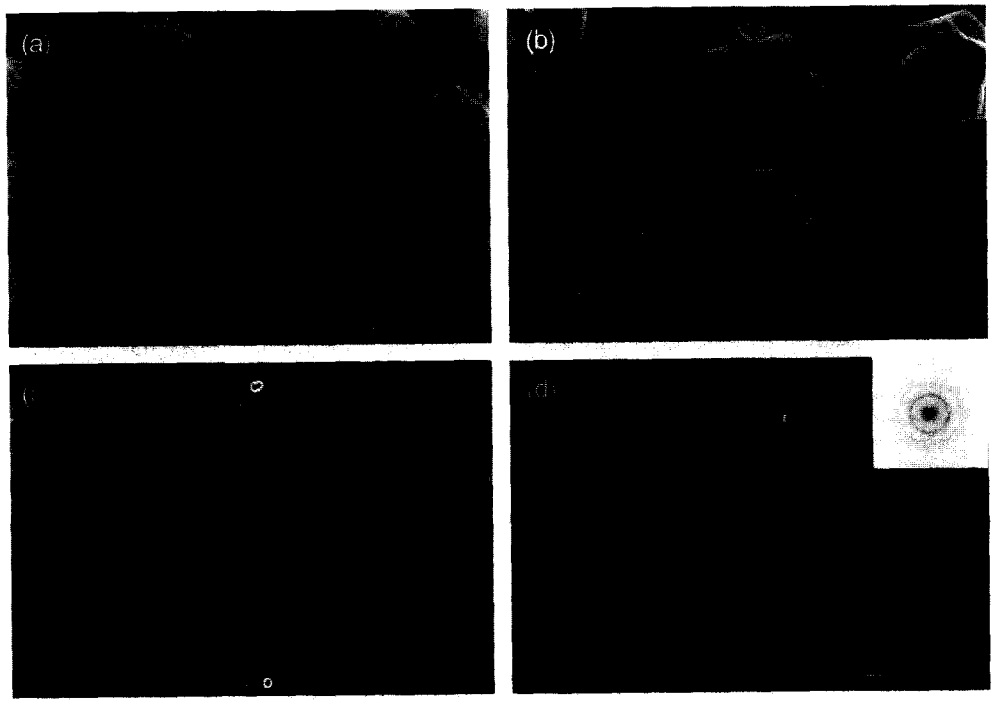

Fig. 2. SEM micrographs of (a) $BaTiO_3$, (b) $BaZrO_3$, (c) $CaTiO_3$ and (d) $CaZrO_3$ powders hydrothermally synthesized at 210°C for 12 h. SADP of $CaZrO_3$ powder is shown at the right upper part of (d).

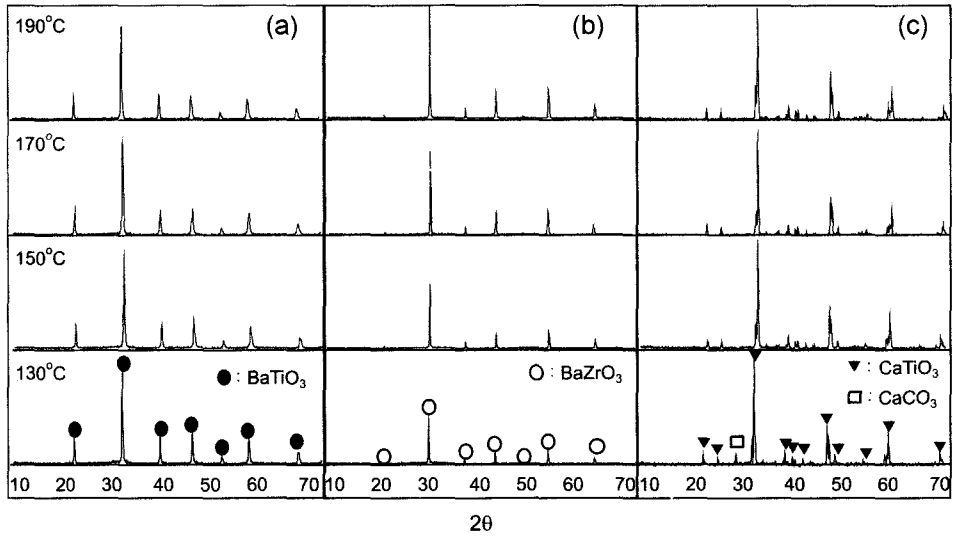

Fig. 3. XRD patterns of hydrothermally synthesized (a) $BaTiO_3$, (b) $BaZrO_3$ and (c) $CaTiO_3$ powders at the given temperatures for 12 h.

structures of each samples were shown in Fig. 2. $BaTiO_3$ powder had an average particle size of ~180 nm. However, each particles were composed of primary particles of 40 nm as was clearly shown in the SEM micrograph of high magnification. In case of $BaZrO_3$, powder had average particle size of ~6 μm and the polyhedral shape of a cubo-octahedron. $CaTiO_3$ had the particle shape of a paper parcel and each sheet seemed to have a orientation relationship each other. On the other hand, $CaZrO_3$ powder had an irregular shape and size. A micro-diffraction pattern of $CaZrO_3$ also showed a typical pattern of amorphous phase.

XRD patterns of the powders synthesized hydrothermally with various temperature are shown in Fig. 3. In case of $BaZrO_3$ powders, the intensity of XRD patterns increased with the reaction temperature. However, the peak intensities of $BaTiO_3$ and $CaTiO_3$ powders were not dependent on the reaction temperature. All of the powders except the $CaTiO_3$ at 130°C that had the unreacted $CaCO_3$ phase as a

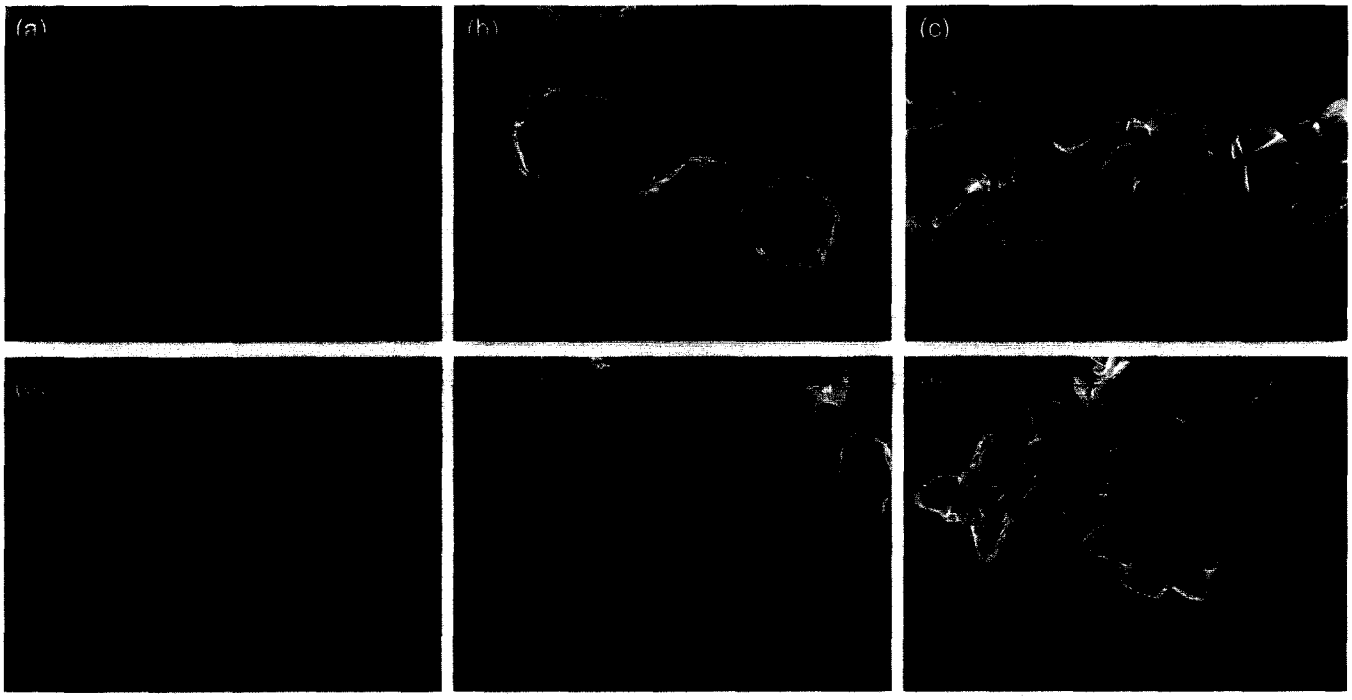

Fig. 4. SEM micrographs of (a) $BaTiO_3$, (b) $BaZrO_3$, (c) $CaTiO_3$ powders synthesized at 130°C for 12 h and (d) $BaTiO_3$, (e) $BaZrO_3$, (f) $CaTiO_3$ powders synthesized at 170°C for 12 h.

second phase showed a crystalline phase. The lowest reaction temperature to synthesize the BCTZ powder was determined to be 150°C. The morphologies of the powders synthesized at the reaction temperature of 130°C and 170°C were shown in Fig. 4.

The $BaTiO_3$ powders obtained were well dispersed and spherical in shape at the given temperature range. The apparent size showed a gradual decrease with increment of the reaction temperature. However, as stated in the previous section, the particles were composed of smaller primary particles. The size of the primary particles was easily determined by the Scherrers formula[18]: $d = 0.9\lambda/B\cos\theta_B$, where d is the primary particle size, λ is the wavelength of $Cu_{K\alpha}$ radiation (0.154056 nm), B is the half-height width of diffraction peak expressed in radian and θ_B is the diffraction angle. Analyses of the XRD peaks for $BaTiO_3$ powders with various reaction temperature showed that primary particle size increased from 25 nm to 40 nm with increment of the reaction temperature from 130°C to 210°C.

The size of the secondary particles is thought to be affected by that of the primary particles. These results can be understood by considering the parameters determining the colloidal stability.[19,20] Typically, the maximum repulsive force can be estimated[21,22] from the equation of $2\pi\varepsilon_0\varepsilon_r k\alpha\Psi^2$ for electrostatically stabilized particles, where ε_0 is the permittivity in free space, ε_r is the dielectric constant of the continuous phase, k is the Debye-Hückel parameter, α is the particle diameter and Ψ is the particle surface potential. Under the constant ionic strength of the solvent, the maximum repulsive force depends on the particle surface potential and the particle size. According to Derjaquin-Landan-Verwey-Overbeek(DLVO) theory,[23] the energy barrier between two particles which inhibit agglomeration can be also expressed as

$$V_b = -(Ak\alpha/12) + 2\pi\varepsilon_0\varepsilon_r k\alpha\Psi^2 \quad (1)$$

where A is the effective Hamaker constant that depends on the dispersion medium. Because the mixed solvent used in this study was composed of water, NH_4OH and KOH in the same ratio, the mixed solvent may not greatly influence the effective Hamaker constants. Under these conditions, therefore, the magnitude of the energy barrier and the maximum repulsive force is determined mainly by the surface potential and the primary particle size.

The result that the apparent particle size of $BaTiO_3$ decrease with the reaction temperature can be interpreted as follows: The potential energy barrier which is given in eq. (1) is higher for the larger primary particles. This means that particles synthesized at high temperature will be more stable against aggregation and, as a result, the apparent particle size was reduced.

On the other hand, in case of $BaZrO_3$, the particle size was observed to increase with the reaction temperature. And the particle morphology was gradually changed from a sphere to a polyhedron as the reaction temperature increased. The shape and size of $CaTiO_3$ particles did not show a tendency with temperature variation while $CaCO_3$ phase formed by unreacted Ca ions was found at the reaction temperature of 130°C. The average particle size measured at the reaction temperature range of 130–210°C was summarized in Table 1.

Table 1. The Average Particle Size of Hydrothermally Synthesized Powders at the Temperature Range of 130–210°C for 12 h.

Composition \ Reaction Temp. (°C)		130	150	170	210
$BaTiO_3$	Primary size (nm)	29	32	35	38
	Secondary size (μm)	0.27	0.24	0.20	0.18
$BaZrO_3$	Particle size (μm)	3.1	4.3	5.2	6.5
$CaTiO_3$	Particle size (μm)	3.5	3.5	3.5	3.5

3.2. Hydrothermal Synthesis of 3-component Systems

A series of hydothermal synthesis were carried out to investigate the extent, y of Zr substitution on Ti sites of $Ba(Ti_{1-y}Zr_y)O_3$. The mixed suspensions that had a composition of y value from 0.1 to 0.9 were synthesized at every 0.1 intervals. NH_4OH and KOH were also used in the same ratio as the prior experiment. All of the peaks in every powder corresponded to a perovskite phase. Another interesting observation made from theses XRD patterns is that the diffraction peaks shifted to a lower angle with the increase in Zirconium content.

Fig. 5 shows the XRD (110) peaks of the stoichiometric $BaTiO_3$ and $BaZrO_3$ and that of the $Ba(Ti_{1-y}Zr_y)O_3$ powders which compositions are 0.1, 0.5 and 0.9 of y value. The shift to a lower angle indicated an increase in the lattice parameter with the addition of Zr ion, which is easily expected from the fact that ionic radius of Zr is larger than Ti ion.[24] Therefore, the gradual replacement of Ti ion by Zr ion correspond

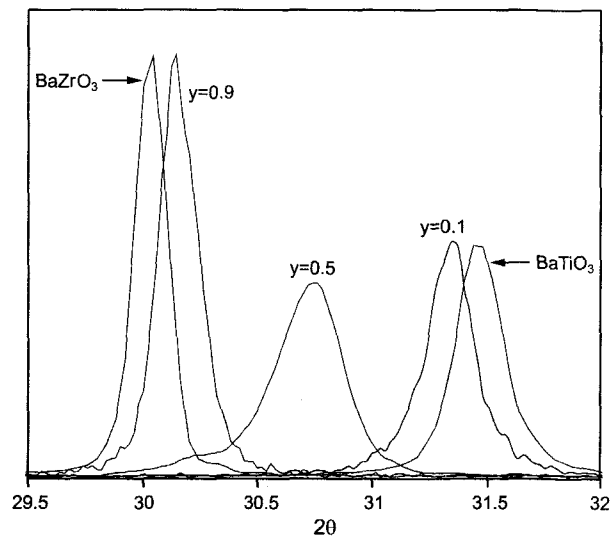

Fig. 5. Dependence of XRD peak shiftness on the Zr substitution of $Ba(Ti_{1-y}Zr_y)O_3$.

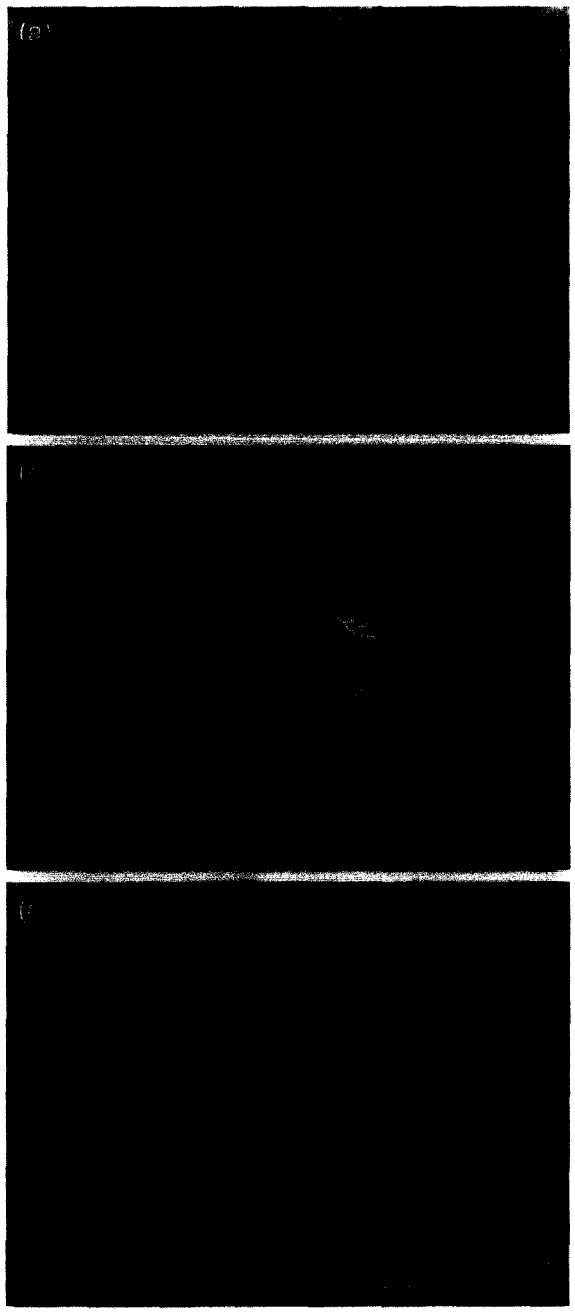

Fig. 6. SEM micrographs of $Ba(Ti_{1-y}Zr_y)O_3$ powders synthesized at 150°C for 12 h with (a) y=0.1, (b) y=0.5 and (c) y=0.9.

to the gradual increase in the lattice parameter in $Ba(Ti_{1-y}Zr_y)O_3$. The morphologies of $Ba(Ti_{1-y}Zr_y)O_3$ powders with various zirconium content were shown in Fig. 6. The morphology of synthesized powders was changed from a small round shape to a large polyhedral one with increase in the Zr content.

In order to determine the solubility limit of Ca ion in $(Ba_{1-x}Ca_x)TiO_3$, the mixed suspensions which had a compositional range of 0.05 and 0.10 in x values were hydrothermally synthesized. There were no peaks except a perovskite phase up

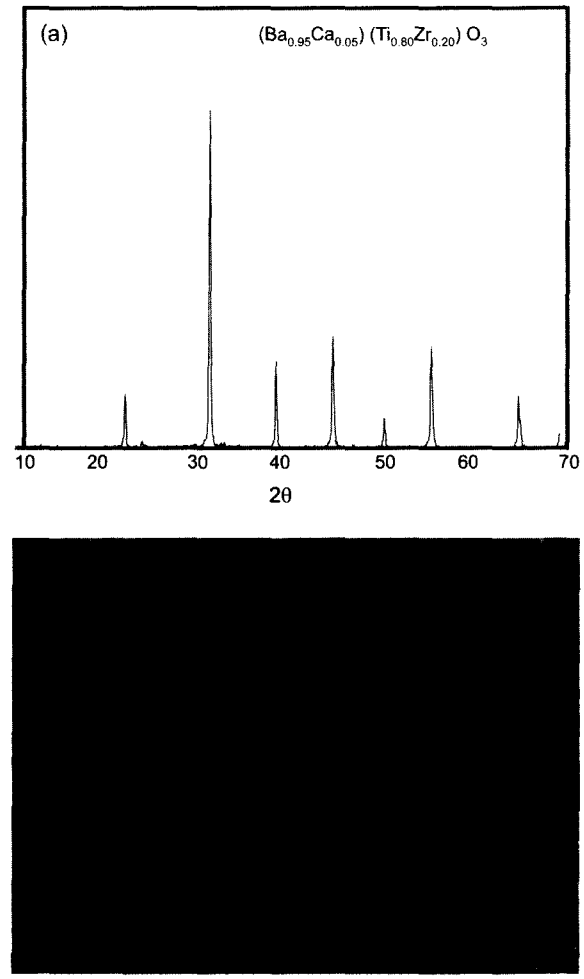

Fig. 7. XRD pattern, (a) and SEM micrograph, (b) of BCTZ powder hydrothermally synthesized at 150°C for 12 h.

to x value of 0.06 in this synthetic condition. However, $CaTiO_3$ peaks began to be found above Ca fraction of 0.07.

3.3. Hydrothermal Synthesis of $(Ba_{0.95}Ca_{0.05})(Ti_{0.80}Zr_{0.20})O_3$ Powder

The target of this study was to get the pure $(Ba_{0.95}Ca_{0.05})(Ti_{0.80}Zr_{0.20})O_3$ powder via hydrothermal synthesis. Through the studies of two and three component systems, the single phase powder of target composition is thought to be synthesized via hydrothermal treatment. As we believed, the single phase BCTZ powder was successfully synthesized under the same condition before. XRD pattern and morphology of BCTZ powder were shown in Fig. 7(a) and (b), respectively. BCTZ powder of a spherical shape had an apparent particle size of ~150 nm.

4. Conclusion

In order to make the pure BCTZ powder, 2 component and 3 component systems were thoroughly investigated. The particles shape and size were dependent on their composi-

tion. The reaction temperature was lowered to 150°C at which $CaCO_3$ would not be formed. Ti and Zr ions are completely soluble to each other and the morphology of $Ba(Ti_{1-y}Zr_y)O_3$ particles were changed from a round shape to a polyhedron with increase in Zr content. And Ca ion can substitute Ba ion up to 6 mol% above which $CaTiO_3$ phase can be precipitated with BCT. We could synthesize the well-dispersed BCTZ powder of ~150 nm size at the reaction temperature of 150°C.

REFERENCES

1. D. F. K. Henning, "Dielectric Materials for Sintering in Reducing Atmospheres," *J. Euro. Ceram. Soc.,* **21** 1637-42 (2001).
2. I. Brun and G. H. Maher, "High Resistivity $BaTiO_3$ Ceramics Sintered in CO-CO_2 Atmosphere," *J. Mater. Sci.,* **10** [4] 633-40 (1975).
3. I. Burn, "Ceramic Disk Capacitors with Base-metal Electrode," *Am. Ceram. Soc. Bull.,* **57** [6] 600-04 (1978).
4. Y. H. Han, J. B. Appleby and D. M. Smith, "Calcium as an Acceptor Impurity in $BaTiO_3$," *J. Am. Ceram. Soc.,* **70** [2] 96-100 (1987).
5. Y. Sakabe, K. Minai and K. Wakino, "High-dielectric Constant Ceramics for Base Metal Monolithic Capacitors(*in Jpn.*)," *Jpn. J. Appl. Phys.,* **20** [4] 147-50 (1987).
6. Y. Hwang, Y. H. Kim and S. J. Park, "The Role of Calcium as a Reduction Inhibitor in $BaTiO_3$," *J. Kor. Ceram. Soc.,* **27** [6] 741-46 (1990).
7. I. Burn, "Mn-doped Polycrystalline $BaTiO_3$," *J. Mater. Sci.,* **14** 2453-58 (1979).
8. W. H. Lee, D. Hennings and Y. C. Lee, "Effect of Dy Doping on Resistance Degreadation of $(Ba)(Ti,Zr)O_3$ Sintered in Reducing Atmosphere under Highly Accelerated Life Test (*in Jpn.*)," *J. Ceram. Soc. Jpn.,* **109** [10] 823-28 (2001).
9. Y. Sakabe, "Dielectric Materials for Base Metal Multilayer Ceramic Capacitors," *Am. Ceram. Soc. Bull.,* **66** [9] 1338-41 (1987).
10. Z. Q. Zhuang, M. P. Harmer, D. M. Smyth and R. E. Newnbam, "The Effect of Octahedrally-coordinated Calcium on the Ferroelectric Transition of $BaTiO_3$," *Mat. Res. Bull.,* **22** 100-03 (1987).
11. D. F. K. Hennings and H. Schreinemacher, "Ca-acceptors in Dielectric Ceramics Sintered in Reducive Atmospheres," *J. Euro. Ceram. Soc.,* **15** 795-800 (1995).
12. I. MacLaren and C. B. Ponton, "A TEM and HREM Study of Particle Formation during Barium Titanate Synthesis in Aqueous Solution," *J. Euro. Ceram. Soc.,* **20** 1267-75 (2000).
13. Ch. Beck, W. Härtl and R. Hempelmann, "Size-controlled Synthesis of Nanocrystalline $BaTiO_3$ by a Sol-gel Type Hydrolysis in Microemulsion-provided Nanoreactors," *J. Mater. Res.,* **13** [11] 3174-80 (1998).
14. W. J. Dawson, "Hydrothermal Synthesis of Advanced Ceramic Powders," *Am. Ceram. Soc. Bull.,* **67** 1673-78 (1988).
15. S. Hirano, "Hydrothermal Processing of Ceramics," *Am. Ceram. Soc. Bull.,* **66** 1342-44 (1987).
16. L. Zhao, A. T. Chien, F. F. Lange and J. S. Speck, "Microstructural Development of $BaiO_3$ Powder Synthesized by Aqueous Methods," *J. Mater. Res.,* **11** [6] 1325-28 (1996).
17. Y. S. Her and E. Matijevic, "Preparation of Well-defined Colloidal Barium Titanate Crystal by the Controlled Double Jet Precipitation," *J. Mater. Res.,* **10** [12] 3106-14 (1995).
18. B. D. Cullity and S. R. Stock, Element of X-Ray Diffraction, 3rd ED., pp. 167-71, Prentice Hall, Inc., New Jersey (2001).
19. I. S. Seog and C. H. Kim, "Preparation of Monodisperse Spherical Silicon Carbide by the Sol-gel Method," *J. Mater. Sci.,* **28** 3277-82 (1993).
20. Y. T. Moon, H. K. Park, D. K. Kim, I. S. Seog and C. H. Kim, "Preparation of Monodisperse and Spherical Zirconia Powders by Heating of Alcohol-aqueous Solutions," *J. Am. Ceram. Soc.,* **78** [10] 2690-94 (1995).
21. J. L. Look and C. F. Zukoski, "Shear Induced Aggregation during the Precipitation of Titanium Alkoxides," *J. Colloid. Interface Sci.,* **153** [2] 469-82 (1992).
22. J. L. Look and C. F. Zukoski, "Colloidal Stability and Titania Precipitate Morphology: Influence of Short-range Repulsions," *J. Am. Ceram. Soc.,* **78** [1] 21-32 (1995).
23. R. J. Hunter, "Foundation of Colloid Science," *Clarendon Press, Oxford, UK,* 443 (1987).
24. Y. Xu, "Ferroelectric Materials and Their Applications," p. 135, North-Holland (1991).